Supporting Information

Single molecule nanopore spectrometry for peptide detection

Amy E. Chavis[1,‡], Kyle T. Brady[1,√], Grace A. Hatmaker[1], Christopher E. Angevine[1], Nuwan Kothalawala[2,†], Amala Dass[2], Joseph W. F. Robertson[3], Joseph E. Reiner[1,*]

1. Department of Physics, Virginia Commonwealth University, Richmond, Virginia 23284, United States.

2. Department of Chemistry and Biochemistry, University of Mississippi, University, Mississippi 38677, United States.

3. Physical Measurement Laboratory, National Institute of Standards and Technology, Gaithersburg, Maryland 20899-8120, United States.

Corresponding Author:

* Joseph E. Reiner, jereiner@vcu.edu

Present Addresses:

‡Bristol-Meyers Squibb, Devens, Massachusetts 01434, United States.
√Naval Surface Warfare Center, Dahlgren Division, Dahlgren, Virginia 22448, United States.
†Eurofins Lancaster Laboratories LLC, Lancaster, PA 17605, United States.

Table of contents

I. Description of the peptides

Leu-enkephalin (LE) is a peptide with a high binding affinity to opioid receptors,[S1-S3] angiotensin I (A1) is a precursor to angiotensin II (A2) which is known to cause blood vessel constriction and a corresponding increase in blood pressure,[S4-S6] Polyglutamine-binding peptide 1 (QBP1) limits polyglutamine protein aggregation that is related to a number of neurodegenerative diseases[S7,S8] and neurotensin (NT) is a ubiquitous neuropeptide.[S9] With the exception of QBP1, each of these peptides is cationic or neutral at the pH values studied throughout this paper. It is worth noting that A1 and A2 contain histidine residues (H) with $pK_a \approx 6$ that makes their charge sensitive to the pH range studied throughout this manuscript. The Z abbreviation in the NT peptide sequence (Table S1 below) corresponds to pyroglutamate, which is a cyclized end group without a titratable amine.

II. Derivation of the Ohmic model-Eq. 1 in the main text

The model highlighted by Eq. 1 in the main text assumes that the ionic current follows from the resistance across the pore from a simple Ohm's law relationship. We neglect the access resistance because the pore length is larger than the pore diameter. When the pore is unoccupied then the open pore current $\langle i_o \rangle$ is given in terms of the applied voltage V, the average cross sectional pore area A_{open}, pore length L_{open} and ionic resistivity ρ_{open} so that

$$\langle i_0 \rangle = \frac{VA_{\text{open}}}{\rho_{\text{open}} L_{\text{open}}}. \tag{S1}$$

When a polymer of average length L_p and cross sectional area A_p partitions into the pore the resistivity in the vicinity of the polymer ρ_p is changed and the resistance can be written as a piecewise linear combination of the unoccupied pore fraction in series with the polymer occluded volume. This leads to the average current through the polymer occupied pore

$$\langle i \rangle = V\left[\frac{\rho_{\text{open}}\left(L_{\text{open}} - L_p\right)}{A_{\text{open}}} + \frac{\rho_p L_p}{A_{\text{open}} - A_p}\right]^{-1}. \tag{S2}$$

Dividing $\langle i \rangle$ by $\langle i_0 \rangle$ leads to an expression for the average magnitude of the current blockades

$$\frac{\langle i \rangle}{\langle i_0 \rangle} = \frac{1}{1 - \left(\frac{L_p}{L_{\text{open}}}\right)\left(1 - \frac{\rho_p}{\rho_{\text{open}}}\left(\frac{1}{1 - A_p/A_{\text{open}}}\right)\right)} \tag{S3}$$

To connect the current blockades to the molecular mass we assume $L_p/L_{\text{open}} = (V_p/V_{\text{open}})^{\nu}$ and $A_p/A_{\text{open}} = (V_p/V_{\text{open}})^{(1-\nu)}$ where V_p and V_{open} are the time-averaged volume of the polymer and open pore respectively and ν is the Flory exponent that parameterizes the polymer geometry in solution.[S10] In addition, we assume peptides studied herein are described by a constant mass density so that $V_p/V_{\text{open}} =$

M_p/M_f where M_p is the mass of the polymer and M_f is the mass of the smallest polymer that completely fills the inside of the pore. Finally, we note that previous efforts with PEG provided a more detailed model connecting cation binding to the polymer with reduction in current.[S11,S12] However, the chemical and structural complexity of peptides precludes the use of this model so we simplify the problem here by introducing a power-law relationship between the resistivity and molecular weight of a given peptide so that $\rho_p/\rho_{open} = a\,(M_p/M_f)^{\gamma}$ where a and γ are adjustable parameters that scale the resistivity to the peptide mass. Resistivity in the vicinity of the peptide ρ_p is affected by ion binding to the peptide.[S11,S12] This implies that $\gamma < 1$ corresponds to hindrance of ion binding to increasing peptide sizes and vice-versa for $\gamma > 1$. Combining these assumptions into Eq. S3 yields the following expression between the mean current blockade induced by a given peptide and that peptide's molecular weight,

$$\frac{\langle i \rangle}{\langle i_0 \rangle} = \frac{1}{1-\left(\frac{M_p}{M_f}\right)^{\nu}\left(1-a\left(\frac{M_p}{M_f}\right)^{\gamma}\left(1-\left(\frac{M_p}{M_f}\right)^{1-\nu}\right)^{-1}\right)}, \tag{S4}$$

which is Eq. 1 in the main text.

III. Calculated effective charge of the peptides

The expected charge of each peptide can be estimated by assuming simple acid-base dissociation of the following form:

$$z_{\text{tot}} = \sum_i N_i \frac{K_{a,i}}{\left[H^+\right] + K_{a,i}} - \sum_j N_j \frac{\left[H^+\right]}{\left[H^+\right] + K_{a,j}} \tag{S5}$$

where i are the $N_{terminus}$ and basic amino acids, (K, R, H) and j are the $C_{terminus}$ and the acidic amino acids (i.e., D,E,C,Y), K_a is the acid dissociation constant, N is the number of component i or j and $[H^+]$ is the activity of protons in solution (i.e., -10^{pH}). Equation S5 assumes each residue is independent of the others. Under high electrolyte concentrations (*e.g.*, 3M), this is a reasonable assumption. Values used for the amino acid $pK_{a,i} = -\log(Ka,i)$ were $N_{terminus}$= 9.69, K=10.67, R=12.10, H=6.04, $C_{terminus}$=2.34, D=3.71, E=4.15, C=8.14, Y=10.10.[S13] Figure S1 shows the calculated charges for A1 and NT referred to in the main text.

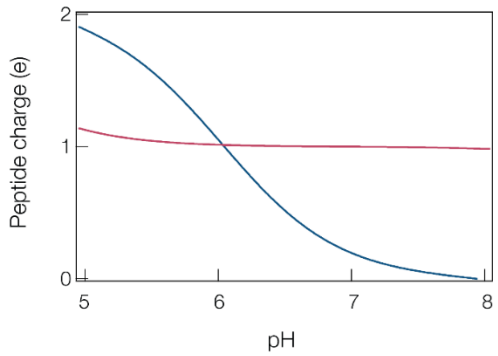

Figure S1: Estimated charge of A1 (blue) and NT (red) calculated from Eq. S5. The A1 has a histidine residue with a $pK_a \approx 6$ that leads to a significant dependence between charge and pH over the range shown. No such residue is present in NT, which makes the charge nearly independent of pH over the same range.

IV. Residence time enhancement: voltage dependence

To find the optimal applied voltage for these experiments we measured the residence time enhancement factor as a function of voltage for the three peptides (A1, A2 and NT). The enhancement factor is defined as the ratio of the gold-occupied mean residence time to the open pore mean residence time. If the charge attraction between the peptide and gold plays an important role in the residence time enhancement, then one would expect the residence time enhancement to increase with increasing voltage because the peptide and cluster would be forced to interact more strongly under a higher magnitude electric field. This was observed for the case of PEG detection[S14] and Figure S2 below shows similar behavior as the enhancement ratio is increased as the applied voltage magnitude increases from 50-70 mV. Beyond 70 mV the enhancement ratio plateaus around 3. This result motivated us to perform all our experiments at a fixed transmembrane voltage of 70 mV to optimize the residence time enhancement.

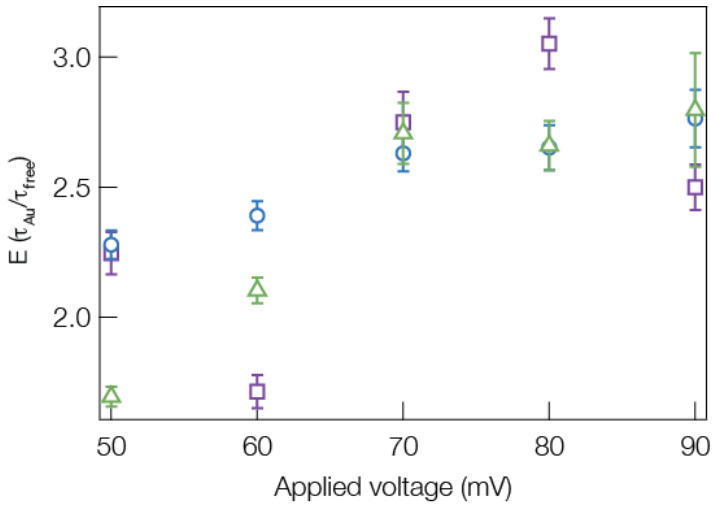

Figure S2: The cationic peptides NT (purple squares), A2 (green triangles) and A1 (blue circles) all show an increase in the mean residence time enhancement ratio ($E = \tau_{gold}/\tau_{open}$) until they plateau around 70 mV. Similar behavior was previously observed for PEG[S14] and suggests a Coloumbic attraction between the cluster and cationic peptide plays a role in the enhancement process.

V. Representative current traces

Long-time current traces illustrate the behavior of the various peptides under near neutral and optimized conditions. Figure S3 shows 60-seconds of current for all the peptides under 70 mV applied transmembrane potential and pH 7.2 solution and Figure S4 shows 60-seconds of data for the A1, A2 and NT peptides under the idealized solution conditions pH 5.8 and 1M Gdm-HCl. From both figures it can be seen that that the gold cluster increases the on-rate of peptides to the pore while also increasing the mean residence time. In addition, these traces also demonstrate the stability of the gold-in-pore states with the exception of the anionic QBP1. This is expected for the QBP1 case because the repulsion between that anionic peptide and the anionic gold clusters should destabilize and "kick-out" gold clusters trapped in the pore vestibule.

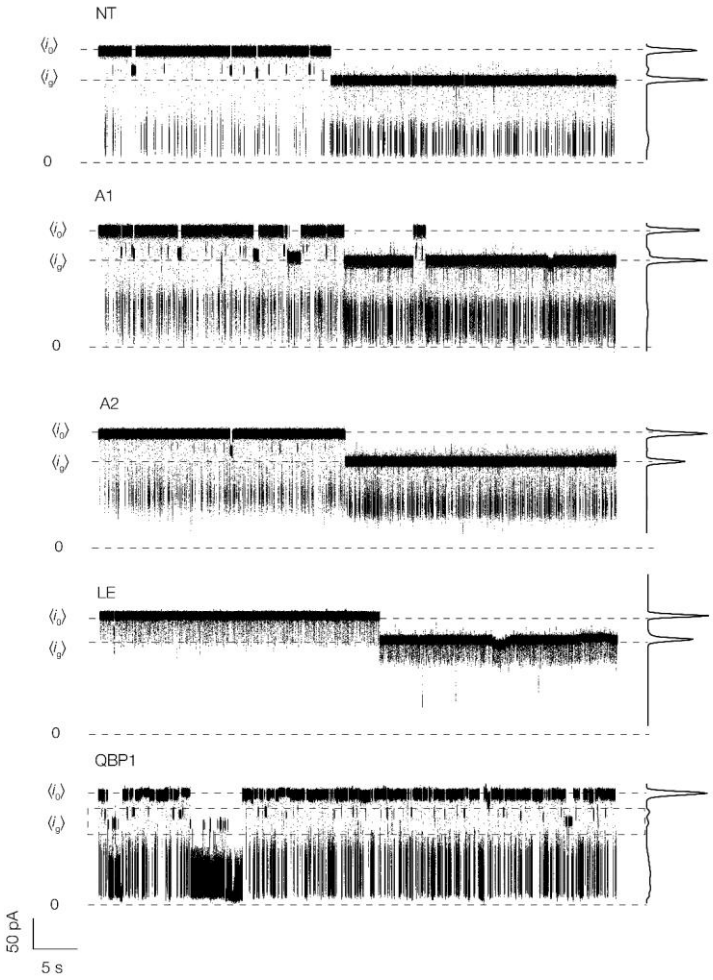

Figure S3: One-minute current traces for the open and gold-occupied pores at pH 7.2 under 70 mV applied transmembrane potential. In each case, except QBP1, the gold increases the on-rate of the peptides. Also, the residence time is increased for all peptides. The vertical distributions to the right of each trace show the corresponding all-points histograms. In each case the gold and open pore states are equally represented except for the QBP1 as expected given the QBP1's tendency to destabilize the anionic gold cluster in the pore.

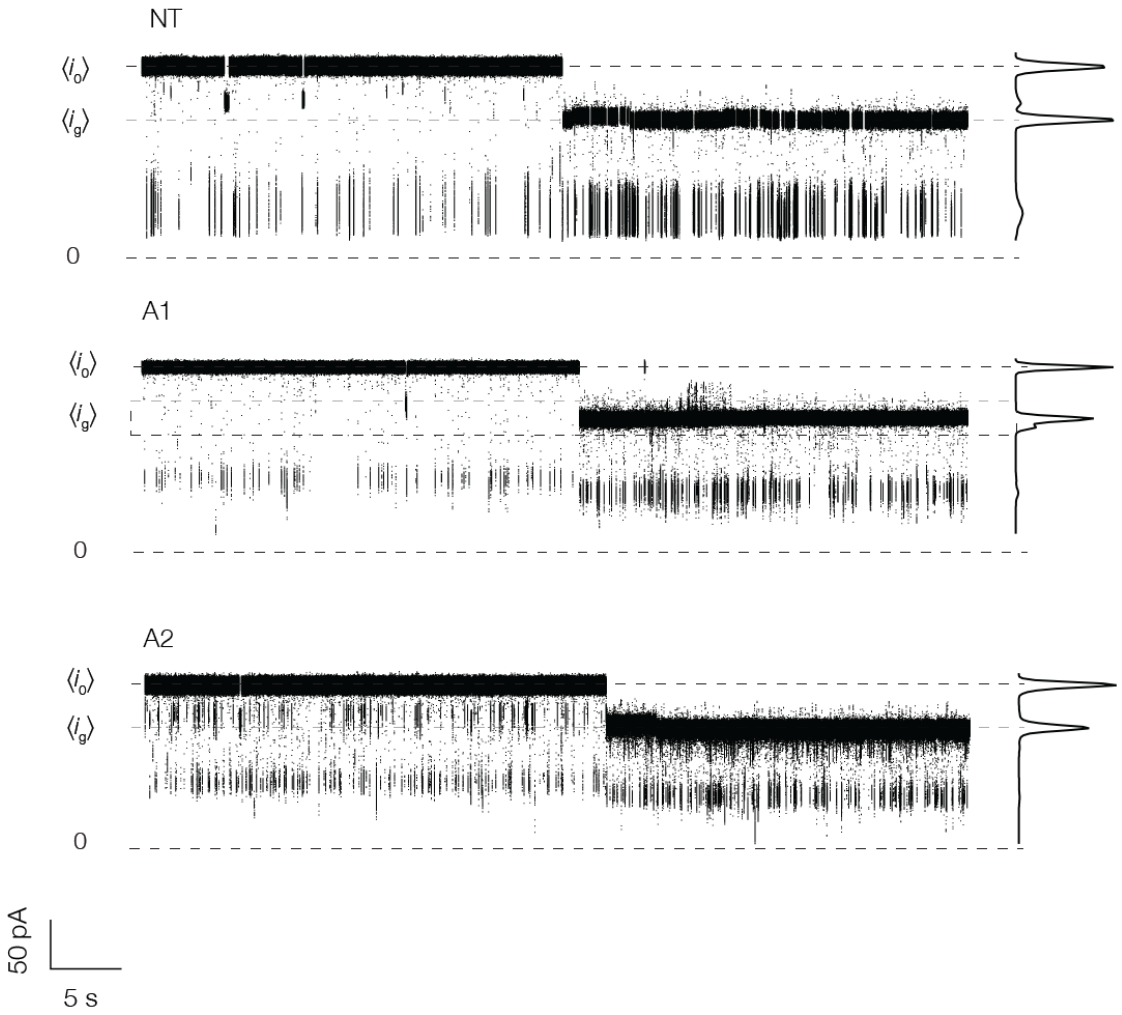

Figure S4: One-minute current traces for the open and gold-occupied pores for the NT, A1 and A2 peptides in the optimized solution conditions (70mV, pH 5.8, 1M Gdm-HCl). As with the traces in Fig. S3, the blockade rate and mean residence time increase when a gold cluster is present in the pore.

VI. Alpha Hemolysin I-V curves with 1M Gdm-HCl on the trans-side of the pore

I-V curves are commonly used to demonstrate the efficacy of the αHL nanopore sensor. To verify that 1M Gdm-HCl on the *trans*-side of the pore has no deleterious effects on the sensor, we present in Figure S5 typical I-V curves both at pH 7.2 and pH 5.8 to show that the nanopore functions well under these conditions.

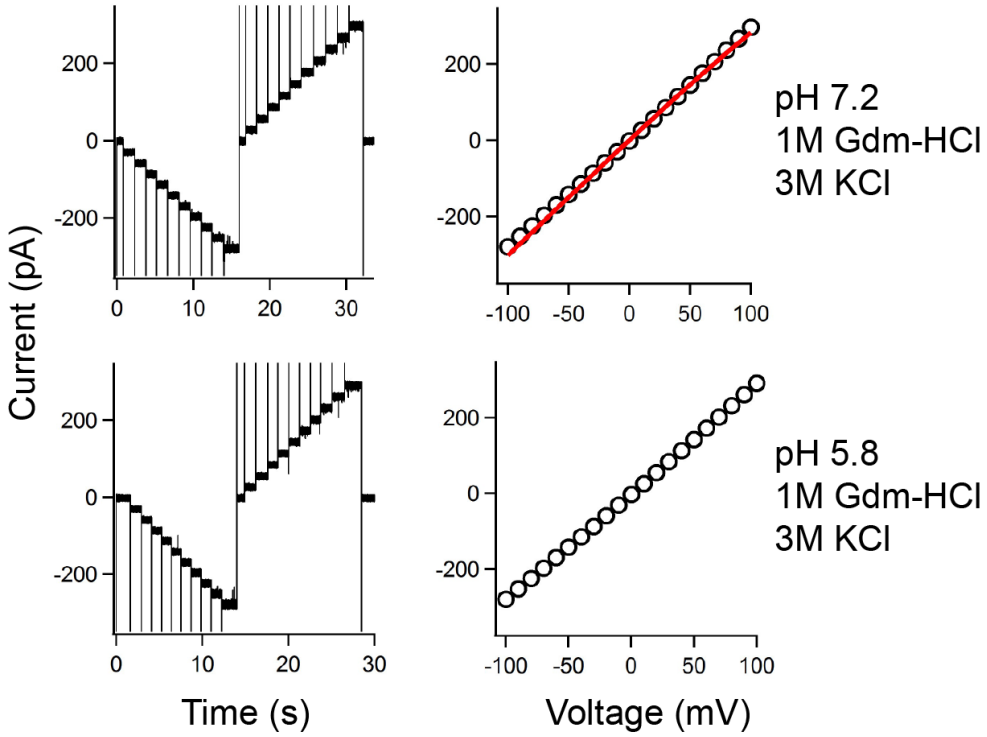

Figure S5: (Left, column) Raw current data traces and (Right, column) corresponding I-V curves (Black circles) at (Top, row) pH 7.2 and (Bottom, row) pH 5.8 with 1M Gdm-HCl added to the *trans*-side of the pore. The current appears stable over the range reported (-100 mV to 100 mV) and the large downward and upward spikes seen in the current trace data correspond to transients from 10 mV voltage jumps applied approximately every 1 second. The pore appears to show little effect from the Gdm-HCl as evidenced by the I-V curve (red line) shown in the upper right plot for pH 7.2 3M KCl with no Gdm-HCl added.

VII. Supplemental data from the main text

Table S1. Summary of water-soluble peptides studied herein.

Peptide	AA Sequence	MW (g/mol)	Charge (e) pH 7.2	Charge (e) pH 5.8
Leu-Enkephalen (LE)	YGGFL	555.62	0.00	0.00
Angiotensin II (A2)	DRVYIHPF	1046.18	+0.06	+0.62
Angiotensin I (A1)	DRVYIHPFHL	1296.48	+0.11	+1.24
QBP1	SNWKWWPGIFD	1435.58	-1.00	-0.99
Neurotensin (NT)	ZLYENKPRRPYIL	1672.92	+1.00	+1.02

Table S2. Summary of the mean blockade depth, peptide on-rate (k_{on}), residence time (τ_{res}), blockade standard deviation (SD), blockade distribution peak widths (FWHM) and corresponding mass resolution (Δm) from Figs. 2 and 3 of the main text. The mass resolution is estimated from the FWHM and the least-squares fitting results of Eqs. 1 and 2 from the main text. Specifically, setting Eq.1 = y_o and Eq. 2 = y_g then Δm(open) = |FWHM(open)/(dy_o/dMp)| and Δm(gold) = |FWHM(gold)/(dy_g/dMp)|. The N/A shown in the QBP1 column denotes the fact that QBP1 led to too few events in the gold-occupied states to enable a well-defined peak in the current blockade distribution. This can be seen in Fig. 2A of the main text. The number of independent experiments used to calculate the reported mean and standard deviations are shown in parenthesis next to the peptide names. Solution conditions were 70 mV, pH 7.2, 3M KCl and [peptide] = 20 μM.

	LE (n = 5)	A2 (n = 6)	A1 (n = 6)	QBP1 (n = 3)	NT (n = 3)
i/i_{open}	0.735 ± 0.019	0.432 ± 0.022	0.339 ± 0.016	0.307 ± 0.024	0.184 ± 0.007
i/i_{gold}	0.744 ± 0.028	0.448 ± 0.022	0.354 ± 0.019	N/A	0.216 ± 0.013
k_{on} (s^{-1}) (open)	5.0 ± 1.8	6.1 ± 2.4	6.7 ± 1.5	7.2 ± 1.4	3.1 ± 0.4
k_{on} (s^{-1}) (gold)	13 ± 5	11 ± 4	11 ± 3	3.8 ± 1.8	6.4 ± 1.3
τ_{res} (ms) (open)	0.019 ± 0.007	0.57 ± 0.29	2.5 ± 0.6	31 ± 8	8.2 ± 1.5
τ_{res} (ms) (gold)	0.036 ± 0.004	1.2 ± 0.6	6.4 ± 1.5	68 ± 2	24 ± 4
SD (pA) (open)	2.2 ± 0.6	11 ± 1	16 ± 3	20 ± 1	11 ± 1
SD (pA) (gold)	2.4 ± 0.9	10 ± 1	14 ± 2	N/A	9.2 ± 0.2
FWHM (open)	0.051 ± 0.010	0.046 ± 0.008	0.040 ± 0.009	0.044 ± 0.003	0.019 ± 0.004
FWHM (gold)	0.064 ± 0.019	0.045 ± 0.011	0.035 ± 0.002	N/A	0.015 ± 0.002
Δm (Da) (open)	69 ± 14	91 ± 16	101 ± 23	128 ± 9	71 ± 15
Δm (Da) (gold)	111 ± 33	95 ± 23	89 ± 5	NA	52 ± 7

Table S3. Summary of the mean residence time (τ_{res}), on-rate (k_{on}), blockade standard deviation (SD), blockade distribution peak width (FWHM) and mass resolution for each condition shown in Fig. 7 from the main text. The number of independent experiments used to calculate the reported mean and standard deviations is shown in parenthesis next to the peptide names. The reported two-fold improvement in mass resolution comes from the weighted average of Δm across all three peptides shown.

Peptide	Condition	τ_{res} (ms)	k_{on} (s^{-1})	SD (pA)	FWHM ($\times 10^{-2}$)	Δm (Da)
A1(6)	pH 7.2 open	2.5 ± 0.6	6.7 ± 1.5	16 ± 3	4.0 ± 0.9	101 ± 23
A1(3)	pH 5.8, gold, 1M Gdm-HCl	7.1 ± 0.5	5.0 ± 1.4	5.6 ± 0.3	1.3 ± 0.1	33 ± 3
A2(6)	pH 7.2 open	0.57 ± 0.29	6.1 ± 2.4	11 ± 1	4.6 ± 0.8	91 ± 16
A2(6)	pH 5.8, gold, 1M Gdm-HCl	1.1 ± 0.5	7.3 ± 1.7	5.9 ± 0.5	3.2 ± 0.4	68 ± 8
NT(3)	pH 7.2 open	8.2 ± 1.5	3.1 ± 0.4	11 ± 1	1.9 ± 0.4	71 ± 15
NT(3)	pH 5.8, gold, 1M Gdm-HCl	35 ± 11	4.3 ± 0.2	9.3 ± 0.5	1.4 ± 0.4	49 ± 14

References:

S1. Frederickson, R. C. A. Enkephalin pentapeptides - A review of current evidence for a physiological role in vertebrate neurotransmission. *Life Sciences* **1977**, *21*, 23-41.

S2. Morley, J. S. Structure-activity relationships of enkephalin-like peptides. *Annu. Rev. Pharmacol. Toxicol*. **1980**, *20*, 81-110.

S3. Deschamps, J. R.; George, C.; Flippen-Anderson, J. L. Structural studies of opioid peptides: a review of recent progress in x-ray diffraction studies. *Biopolymers* **1996**, *40*, 121-139.

S4. Weir, M. R.; Dzau, V. J. The renin-angiotensin-aldosterone system: a specific target for hypertension management. *Am. J. Hypertens*. **1999**, *12*, 205S-213S.

S5. Baker, K. M.; Booz, G. W.; Dostal, D. E. Cardiac actions of angiotensin II: Role of an intracardiac renin-angiotensin system. *Annu. Rev. Physiol*. **1992**, *54*, 227-241.

S6. Paul, M.; Poyan Mehr, A.; Kreutz, R. Physiology of local renin-angiotensin systems. *Physiol. Rev*. **2006**, *86*, 747-803.

S7. Popiel, H. A.; Burke, J. R.; Strittmatter, W. J.; Oishi, S.; Fujii, N.; Takeuchi, T.; Toda, T.; Wada, K.; Nagai, Y. The Aggregation Inhibitor Peptide QBP1 as a Therapeutic Molecule for the Polyglutamine Neurodegenerative Diseases. *J. Amino Acids* **2011**, *2011* 265084.

S8. Sciarretta, K. L.; Gordon, D. J.; Meredith, S. C. Peptide-based inhibitors of amyloid assembly. *Methods Enzymol*. **2006**, *413*, 273-312.

S9. Tyler-McMahon, B. M.; Boules, M.; Richelson, E. Neurotensin: peptide for the next millennium. *Regul. Pept*. **2000**, *93*, 125-136.

S10. Flory, P. J. The configuration of real polymer chains. *J. Chem. Phys*. **1949**, *17*, 303-310.

S11. Reiner, J. E.; Kasianowicz, J. J.; Nablo, B. J.; Robertson, J. W. F. Theory for polymer analysis using nanopore-based single-molecule mass spectrometry. *Proc. Natl. Acad. Sci. USA* **2010**, *107*, 12080-12085.

S12. Balijepalli, A.; Robertson, J. W. F.; Reiner, J. E.; Kasianowicz, J. J.; Pastor, R. W. Theory of polymer-nanopore interactions refined using molecular dynamics simulations. *J. Am. Chem. Soc*. **2013**, *135*, 7064-7072.

S13. "Properties of Amino Acids," in *CRC Handbook of Chemistry and Physics*, 97th Edition (Internet Version 2017), W. M. Haynes, ed., CRC Press/Taylor & Francis, Boca Raton, FL.

S14. Chavis, A. E.; Brady, K. T.; Kothalawala, N.; Reiner, J. E. Voltage and blockade state optimization of cluster-enhanced nanopore spectrometry. *Analyst*, **2015**, *140*, 7718-7725.